FULL LENGTH ARTICLE

Corrosion protection of mild steel by a new phosphonate inhibitor system in aqueous solution

M. Prabakaran, K. Vadivu, S. Ramesh *, V. Periasamy

Department of Chemistry, The Gandhigram Rural Institute, Deemed University, Gandhigram, 624302 Dindigul, Tamilnadu, India.

Abstract A protective film has been developed on the surface of the mild steel in low chloride aqueous environment using a synergistic mixture of an eco friendly inhibitor, imino dimethyl phosphonic acid (IDMPA) and Zn^{2+}. The synergistic effect of IDMPA in controlling corrosion of the mild steel has been investigated by gravimetric and electrochemical studies in the presence of Zn^{2+}. The formulation consisting of IDMPA and Zn^{2+} has excellent inhibition efficiency. The mixed mode of inhibition studied by potentiodynamic polarization and electrochemical impedance spectroscopy has shown that the changes in the impedance parameters like charge transfer resistance (R_{ct}) and constant phase element (CPE) confirm the strong adsorption on the mild steel. Surface characterization inspection using Fourier transform infrared (FTIR) spectroscopy, scanning electron microscopy (SEM) and energy-dispersive X-ray spectroscopy (EDS) is used to ascertain the nature of the protective film. The mechanistic aspects of corrosion inhibition are proposed.

© 2014 Production and hosting by Elsevier B.V. on behalf of Egyptian Petroleum Research Institute.

1. Introduction

Mild steel is widely applied as a construction material in many chemical and petrochemical industries due to its excellent mechanical properties and low cost. Corrosion is the destruction or deterioration of metals. Corrosion in cooling water systems greatly affects the health of human beings and economic level of the world. One of the most practical methods for protection against excessive dissolution of metal by corrosion is the use of proper inhibitors [1]. Inhibitors are extremely effective even in very small concentrations and effectively reduce the corrosion rate. The technique of adding inhibitors to the environment of a metal is a well known method of controlling corrosion in many branches of technology. Among various inhibitors, phosphonates were considered as scale inhibitors at the beginning, later they were proved to be good corrosion inhibitors in nearly neutral aqueous media [2]. The inhibition of molecule depends on the nature of the charge distribution and the interaction between the metal surface and the inhibitor molecule and number of adsorption sites available.

Phosphonates have been extensively used as water treatment agents because of their low toxicity, high stability and corrosion inhibition activity in neutral aqueous media [3,4]. The reason for choosing phosphonate as an inhibitor is its property of adsorption on the metal surface, thereby forming

* Corresponding author.
E-mail addresses: prabakar05@gmail.com (M. Prabakaran), drsramesh_56@yahoo.com (S. Ramesh).
Peer review under responsibility of Egyptian Petroleum Research Institute.

poorly soluble compounds and thus decreases the area of active metal surface or by increase in the activation energy. Thus, the corrosion rate is decreased, which proves that corrosion in aqueous media is an electrochemical process.

Phosphonates have high hydrolysis stability and they cannot be easily degraded by microorganisms. In phosphonate based inhibitor system, the inhibition efficiency was increased by the addition of metal cations like Ca^{2+}, Mg^{2+}, Zn^{2+}, Ni^{2+}, Co^{2+}, Cd^{2+}, Mn^{2+}, Sn^{2+}, Cu^{2+}, Fe^{2+}, Ba^{2+}, Sr^{2+}, Al^{3+}, Cr^{3+} etc., in nearly neutral media. In the above series zinc was chosen as the good metal ion to enhance the inhibition property of phosphonates [5,6].

Donor–acceptor interaction between the metal and inhibitor forms a thin protective layer (chemisorption binding) on the metal surface that reduces the corrosion rate. Here the phosphonates act as the surfactant and are diprotic in nature, their properties are studied on the basis of polar head groups. Several corrosion inhibition studies have been carried out using phosphonic acids viz., aminotris (methylene phosphonic acid) (ATMP) [7], 1-hydroxyethane-1,1-diphosphonic acid (HEDP) [8], piperidin-1-yl-phosphonic acid (PPA) [9], 2-carboxy ethyl phosphonic acid (2-CEPA) [10], carboxy methyl phosphonic acid (CMPA) [11], propyl phosphonic acid [12], 2-chloroethyl phosphonic acid (2-ClEPA) [13], 4-phosphono-piperazin-1-yl-phosphonic acid (PPPA) [14], 2-phosphonobutane-1,2,4-tricarboxylic acid (PBTC) [15], phosphonate anions [16] and so many other corrosion inhibitors that have been reported in the literature. Compounds with a phosphonic functional group are considered to be the most effective chemicals for inhibiting the corrosion process and it is well known that short-chain substituted phosphonic acids are good corrosion inhibitors for iron and low alloyed steels.

In the present work, the inhibitive effect of using a new organic inhibitor viz., imino dimethyl phosphonic acid (IDMPA) and Zn^{2+} ions in controlling the corrosion of the mild steel in neutral aqueous environment containing low chloride has been studied by non electrochemical and electrochemical studies such as: potentiodynamic polarization and impedance spectroscopy. Surface analytical techniques, viz., Fourier transform infrared spectroscopy (FTIR), and scanning electron microscopy (SEM) with energy dispersive X-ray analysis (EDX) were used to investigate the nature of protective film formed on the metal surface. A plausible mechanism of inhibition of corrosion is proposed. For all these studies, aqueous solution of 60 ppm chloride has been chosen as control because the water used in cooling water systems is generally either demineralized water or unpolluted surface water.

2. Experimental

2.1. Materials

The molecular structure of the IDMPA is shown in Fig. 1. The tested compound namely imino dimethyl phosphonic acid (IDMPA) obtained from Sigma-Aldrich was used without further purification. Zinc sulfate ($ZnSO_4 \cdot 7H_2O$), sodium chloride and other reagents were analytical grade chemicals. All the solutions were prepared using triple distilled non-deaerated water.
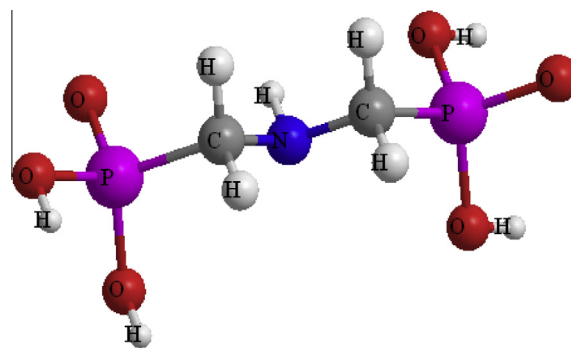
Figure 1 Molecular structure of imino dimethyl phosphonic acid (IDMPA).

2.2. Preparation of specimens

Mild steel specimens (0.026% S, 0.035% P, 0.58% Mn, 0.104% C and the rest iron) of dimensions 3.5 cm × 1.5 cm × 0.2 cm, were polished to a mirror finish with 1/0, 2/0, 3/0, 4/0, 5/0, and 6/0 emery polishing papers respectively, degreased with acetone, dried and used for gravimetric measurements, FTIR and SEM for surface studies. The dimensions of the specimens with 1.0 cm × 1.0 cm and 0.2 cm thickness of the electrode were encapsulated by araldite paste and the effective exposed surface area of 1 cm^2 was used for electrochemical studies

2.3. Gravimetric studies

Gravimetric experiments are the classical way to find the corrosion rate (CR) and inhibition efficiency (IE). In all gravimetric experiments, the polished specimens were weighed and immersed in duplicate, in 100 ml in the absence (control solution) and presence of inhibitor formulations of different concentrations, for a period of 7 days and pH 7.0 was maintained for all test solutions. Then, the specimens were reweighed after washing and drying. The weights of the specimens before and after immersion were determined with Mettler electronic balance AE 240 model with a readability of 0.1 mg. Accuracy in weighing up to 0.0001 g and its surface area measurement up to 0.1 cm^2, as recommended by ASTM, was followed. Corrosion rates of the mild steel in the absence and presence of various inhibitor formulations are expressed in milligram per dm^2 per day (mdd). The corrosion rate was calculated according to the following equation:

$$CR \ (mdd) = \left[\frac{\Delta W}{St} \right] \times 100 \qquad (1)$$

where ΔW (mg) is the weight loss, S (dm^2) is the surface area and t (days) is the immersion period. Inhibition efficiencies (IE) of the inhibitor were calculated by using the formula

$$IE_g \ (\%) = \left[\frac{CR_0 - CR_I}{CR_0} \right] \times 100 \qquad (2)$$

where CR_0 and CR_I are the corrosion rates in the absence and presence of inhibitor, respectively.

2.4. Electrochemical studies

The electrochemical experiments viz., potentiodynamic polarization and electrochemical impedance spectroscopy, were carried out using CHI Electrochemical analyzer model 760D with operating software CHI 760D. The analyzer had a three electrode cell setup having a mild steel working electrode embedded in a Teflon holder with exposed surface area of 1.0×1.0 cm in corrosive environment, a saturated calomel electrode (SCE) as reference electrode, and a platinum wire as counter electrode. The reference electrode was placed close to the working electrode to minimize IR contribution. Before each potentiodynamic polarization and electrochemical impedance study, the electrode was allowed to corrode freely and its open circuit potential (OCP) was recorded as a function of time up to 30 min. After this time, the steady state, corresponding to the corrosion potential of the working electrode, was obtained. The potentiodynamic polarization measurements were started from cathodic to the anodic direction (OCP $\pm$ 200 mV) with a scan rate of 1 mV s^{-1} and the parameters such as corrosion potential (E_{corr}), corrosion current density (I_{corr}) and anodic Tafel slope (β_a) and cathodic Tafel slope (β_c) were obtained by the Tafel extrapolation method. The inhibition efficiencies (IE$_P$) were calculated from I_{corr} values using the following relation

$$IE_P \ (\%) = \left[\frac{I_{corr} - I'_{corr}}{I_{corr}}\right] \times 100 \qquad (3)$$

where I_{corr} and I'_{corr} are the corrosion current densities in case of the control and inhibitor solutions respectively.

Electrochemical impedance spectroscopy measurements were carried out using ac signals of amplitude 5 mV peak to peak in the frequency range from 10,000 Hz to 0.1 Hz. The electrochemical parameters such as charge transfer resistance (R_{ct}), constant phase element (CPE) and constant exponent (n) were calculated from EIS studies. The inhibition efficiencies (IE$_I$) were calculated using the following equation,

$$IE_I \ (\%) = \left[\frac{R'_{ct} - R_{ct}}{R'_{ct}}\right] \times 100 \qquad (4)$$

where R_{ct} and R'_{ct} are the charge transfer resistance values in the absence and presence of the inhibitor respectively.

2.5. Surface evaluation studies

The nature of the film formed on the surface of the metal specimen was analyzed by Fourier transform infrared spectroscopy (FTIR), scanning electron microscopy (SEM) and energy dispersive X-ray spectroscopy (EDX).

2.5.1. Fourier transform infrared (FTIR) spectra
FT-IR spectra were recorded with a frequency ranging from 4000 to 400 cm^{-1} with a resolution of 4 cm^{-1} for the inhibitor as well as the inhibitor adsorbed on the mild steel in aqueous solution in KBr matrix using an FT-IR JASCOW 460 plus model instrument.

2.5.2. Scanning electron microscopy
The polished mild steel specimens were immersed in 60 ppm chloride solutions in the absence and in the presence of the inhibitor. After 7 days, the specimens were taken out, washed with distilled water and dried. The SEM photographs of the surfaces of the specimens were investigated using a JEOL model JSM-5500. The energy of the acceleration beam employed was 20 kV.

2.5.3. Energy dispersive analysis of X-rays (EDX)
EDX system attached with a JEOL JSM-5500 scanning electron microscope was used for elemental analysis or chemical characterization of the film formed on the mild steel surface before and after applying the inhibitor.

2.6. Quantum chemical calculations

The quantum chemical calculations were carried out using Jaguar module of Schrodinger. Complete geometry optimization was carried out using density functional theory (DFT) with Becke's three-parameter exchange potential and Lee–Yang–Parr correlation functional (B3LYP), using basis set 3-21* level using PBF salvation.

3. Results and discussion

3.1. Evaluation of corrosion inhibition

3.1.1. Gravimetric measurements
The gravimetric measurements were carried out to calculate the corrosion rate (CR) and inhibition efficiency (IE) for the mild steel in an aqueous solution containing 60 ppm chloride ions (control solution) in the absence and presence of various concentrations of the IDMPA (10–250 ppm) and Zn^{2+} (10–50 ppm) for 7 day immersion periods. Inhibition efficiency and corrosion rate obtained from gravimetric measurements at different concentrations of inhibitor for the corrosion of the mild steel immersed in control solution, in the absence and presence of Zn^{2+} are given in Table 1. The results of the gravimetric studies using the binary system IDMPA–Zn^{2+} at various concentrations of both constituents are shown in Fig. 2. Initially the mild steel corroded in control solution and showed very high corrosion rate with heavy metal loss. The corrosion rate decreased and the inhibition efficiency increased appreciably by addition of 50 ppm Zn^{2+} and 100 ppm IDMPA and the efficiency reached up to 99%. It is evident from gravimetric results that IDMPA by itself is a poor corrosion inhibitor and Zinc ions are found to be corrosive. However, interestingly IDMPA–Zn^{2+} combination offers a good corrosion inhibitor system. The formulation consisting of 10 ppm Zn^{2+} and 100 ppm IDMPA shows an inhibition efficiency of 54%. On increasing concentration of Zn^{2+} from 20 ppm to 50 ppm, the inhibition efficiencies also increase to 92%, 97%, and 99% respectively. The combination containing 50 ppm of Zn^{2+} and 100 ppm of IDMPA has achieved the maximum inhibition efficiency (IE) of 99%. In this way, a synergistic corrosion inhibition effect is noticed. It is found that the value of inhibition efficiency was increased with an increase in the concentration of Zn^{2+}. After this concentration, no appreciable change in efficiency was observed. It can be interpreted that low concentrations of Zn^{2+} are insufficient to form a protective film with IDMPA on the metal surface. At lower

Table 1 Inhibition efficiency (%) obtained by gravimetric studies of the mild steel in absence and presence of inhibitor (IDMPA–Zn^{2+}).

IDMPA (ppm)	Zn^{2+} (ppm)											
	0		10		20		30		40		50	
	CR	IE	CR	IE	CR	IE	CR	IE	CR	IE	CR	IE
0	13.32	-	13.19	1	13.05	2	12.65	5	12.25	8	11.85	11
10	11.72	12	9.22	31	9.01	32	8.77	34	7.80	40	10.34	20
25	11.46	14	6.21	53	8.98	33	3.60	73	4.28	68	8.73	34
50	11.19	16	9.08	32	7.47	44	3.29	75	3.97	70	7.15	46
75	11.06	17	9.76	27	7.57	43	3.07	77	1.21	90	0.99	93
100	9.99	25	6.11	54	8.42	37	1.07	92	0.36	97	**0.18**	**99**
150	10.12	24	4.86	63	7.04	47	0.72	95	0.99	93	0.09	99
200	10.66	20	8.11	39	5.99	55	0.54	96	1.29	90	0.09	99
250	11.06	17	3.72	38	7.30	45	0.75	94	1.07	92	0.27	98
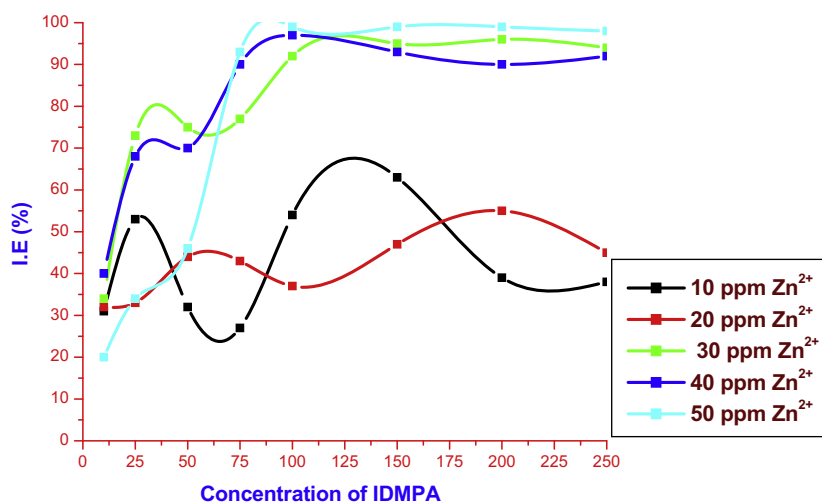
Figure 2   Inhibition efficiency as a function of concentration of IDMPA.

concentrations of Zn^{2+}, the IDMPA is precipitated as IDMPA–Zn^{2+} complex in the bulk of the solution and not transported toward the metal surface. The synergistic combination of 50 ppm Zn^{2+} and 100 ppm IDMPA offered the maximum inhibition efficiency of 99%. The anodic reaction is controlled by the formation of Fe^{2+}–IDMPA complex on the sites of the metal surface. The cathodic reaction is controlled by the formation of $Zn(OH)_2$ on the cathodic sites of the metal surface.

3.1.2. Effect of pH

The influence of pH on corrosion rate of the mild steel in the presence of inhibitor system and the maximum inhibition efficiency obtained in the gravimetric measurements were studied. The effect of pH for the synergistic formulation consisting of IDMPA (100 ppm) + Zn^{2+} (50 ppm), in the pH range of 3–11 is shown in Fig. 3. It is evident from the results obtained that the inhibition efficiency decreases on increasing the pH from 7.0 to 9.0 in alkaline medium and also on decreasing the pH from 5.0 to 3.0. The highest inhibition efficiency could be obtained in the pH range of 5.0 to 7.0. However, interestingly, the corrosion inhibition efficiency again increases from pH 10.0 to 11.0. This is due to the formation of sodium zincate
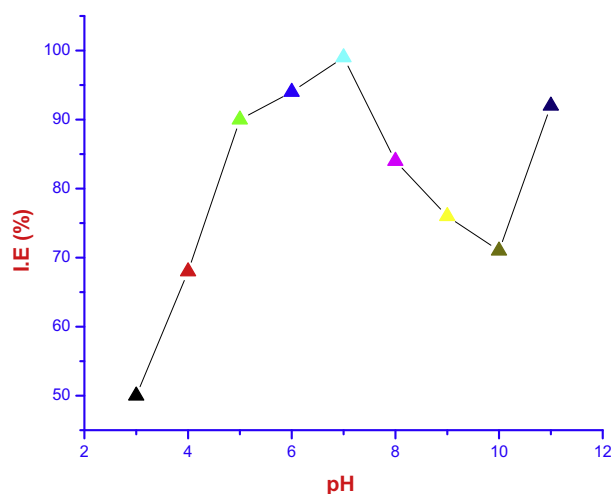
Figure 3   Effect of pH.

over the metal surface, protecting the metal due to metal passivation. This inhibitor formulation is effective in the pH range of 5.0 to 7.0 and also at pH 11.0.

3.2. Electrochemical impedance spectroscopy (EIS)

EIS measurements were carried out to determine the kinetic parameters for electron transfer reactions at the iron/electrolyte interface [17]. The corrosion behavior of the mild steel in aqueous solution containing 60 ppm Cl^- (control solution) with and without inhibitor was also investigated by EIS measurements. The impedance parameters derived from these plots are given in Table 2 and Fig. 4 which show the impedance behavior of the mild steel corrosion in the form of Nyquist plots.

Double layer capacitance (C_{dl}) and charge transfer resistance values (R_{ct}) were obtained from impedance measurements. In the case of the electrochemical impedance spectroscopy, inhibition efficiency (IE_I) is calculated by charge transfer resistance using Eq. (4). The double layer capacitance (C_{dl}) and the frequency at which the imaginary component of the impedance is maximum ($-Z_{max}$) are represented in the equation

$$C_{dl} = 1/\omega R_{ct} \qquad (5)$$

where $\omega = 2\pi/max$.

From Nyquist plots in Fig. 4, it is clear that the impedance diagrams in most cases do not show a perfect semicircle. This behavior can be attributed to the frequency dispersion [18,19] as a result of homogenates of the electrode surface. These curves are dispersed in nature. Also these curves show a single semicircle indicating the occurrence of a single charge transfer reaction. All the Nyquist plots obtained in the present study are characterized by single time constant. Fig. 5 shows the equivalent circuit based on the EIS data. Such an equivalent circuit was also discussed by several researchers [20–22] who obtained similar depressed semicircles with single time constant. In this equivalent circuit, R_s is the solution resistance between the reference and working electrode, R_{ct} is the charge transfer resistance corresponding to corrosion reaction at metal/electrolyte interface and CPE is the constant phase element. CPE is substituted for the respective capacitor of C_{dl} in order to fit the depressed semicircles better [23].

The impendence of CPE is defined as

$$Z_{CPE} = Y_0^{-1}(j\omega)^{-n} \qquad (6)$$

where Y_0 is the modulus, j is the imaginary root; ω is the angular frequency and n is the phase [24]. Depending on the value of exponent n, Z_{CPE} represents a resistance with $R = Y^{-1}$; for $n = -1$, an inductance with $C = Y$ [25]. The value range of a real electrode of n is often between 0 and 1. The smaller the value of n, the rougher the electrode surface and the more serious, the corrosion of the electrode [26].

In the present study, in the presence of the control alone, a small semicircle with an R_{ct} value of 125 Ω is observed. A sim-
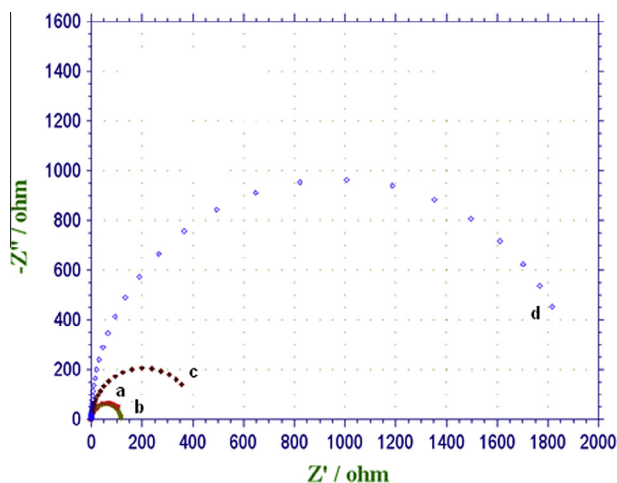
Figure 4a Nyquist plots of mild steel immersed in various test solutions: (a) Control solution (60 ppm Cl^-); (b) 50 ppm Zn^{2+}; (c) 100 ppm IDMPA; (d) 100 ppm IDMPA + 50 ppm Zn^{2+}.
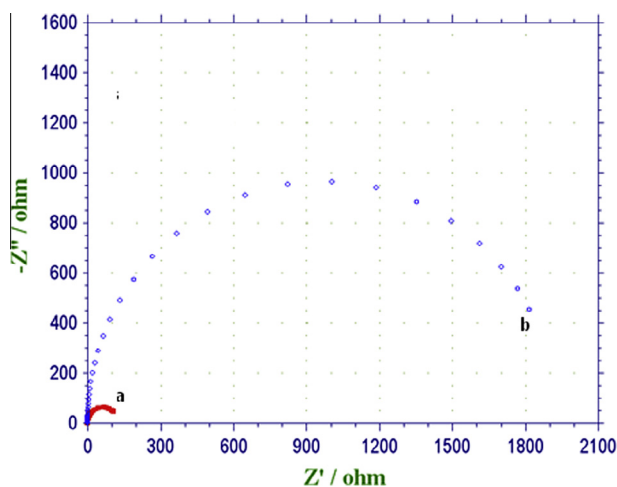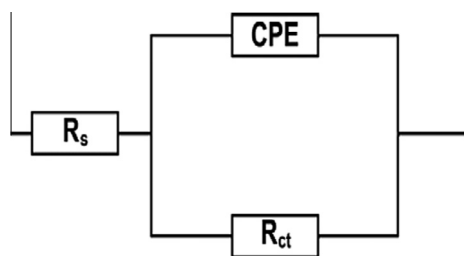

Figure 4b Nyquist plots of mild steel immersed in various test solutions: (a) Control solution (60 ppm Cl^-); (b) 100 ppm IDMPA + 50 ppm Zn^{2+}.

ilar semicircle is also obtained when 50 ppm of Zn^{2+} is added to the control. Due to Zn^{2+}, R_{ct} is decreased and C_{dl} value is increased in the value of n. These changes are due to the replacement of water molecules in the interface by Zinc ions, which resulted in the increased rate of corrosion. By the addition of 100 ppm of IDMPA to the control, a slightly depressed semicircle with high R_{ct} value is obtained. The

Table 2 A.C. impedance parameters obtained for the mild steel immersed in the absence and presence of inhibitor.

Concentration (ppm)		Charge transfer resistance R_{ct} (Ω)	Double layer capacitance C_{dl} ($\mu F/cm^2$)	Constant exponent n	IE (%)
IDMPA	Zn^{2+}				
0	0	125	20.34	0.59	–
100	0	409	1.87	0.60	69
0	50	117	22.97	0.86	–
100	50	1936	0.085	0.84	94

Figure 5 Nyquist plots are fitted by the equivalent electrical circuit.

Figure 6a Potentiodynamic polarization curves of mild steel immersed in various test solutions: (a) Control solution (60 ppm Cl^-); (b) 100 ppm IDMPA; (c) 50 ppm Zn^{2+}; (d) 100 ppm IDMPA + 50 ppm Zn^{2+}.

capacitance value is decreased from 20.34 μF/cm^2 to 1.87 μF/cm^2 and n value is increased. These observations can be attributed to the presence of inhibitor molecules in the double layer and the control of corrosion process to some extent. When the combination of 50 ppm Zn^{2+} and 100 ppm IDMPA is considered, a large depressed semicircle is observed from high frequency to low frequency regions. The R_{ct} becomes dominant in the corrosion process due to the presence of the inhibitor molecule to form a protective film on the metal surface. This result is supported by the significant decrease in C_{dl} and increase in n value. The binary formulation (IDMPA–Zn^{2+}) represents an R_{ct} value of 1936 Ω which is greater than that observed in case of the control. The C_{dl} value at the metal/solution interface is found to decrease from 20.34 μF/cm^2 in the case of the control to 0.085 μF/cm^2 in the case of the binary inhibitor formulation. The value of n is considerably increased to 0.84 in the presence of the binary inhibitor system, suggesting a decrease in inhomogeneity of the interface during inhibition. All these results indicate that there is formation of a protective film in the presence of the binary inhibitor formulation and several authors who studied the inhibiting effects of phosphonate based corrosion inhibitors also reported that there is formation of a thick and less permeable protective film on the metal surface [27–29]. They also concluded that the protective film consists of phosphonate–metal complexes. The impedance result of the present study also implies the synergistic action operating between IDMPA and Zn^{2+}. This is in agreement with the inferences drawn from gravimetric studies.
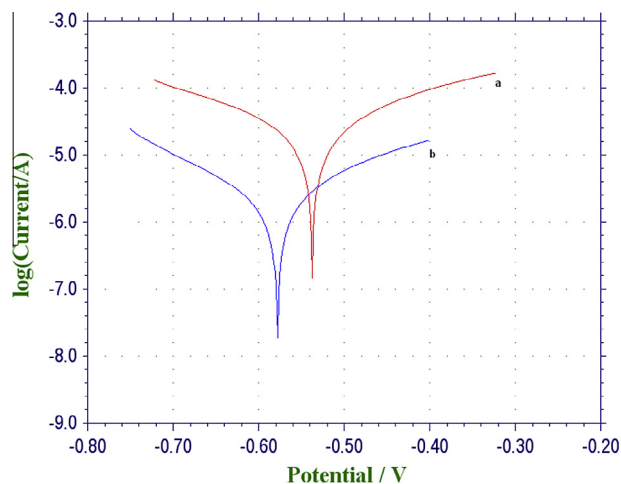
3.3. Potentiodynamic polarization studies

The Tafel parameters derived from these curves and the inhibition efficiencies are listed in Table 3. The potentiodynamic polarization curves of the mild steel electrode in solution containing 60 ppm Cl^- at pH 7 in the absence and presence of various inhibitor combinations are shown in Fig. 6.

The corrosion potential (E_{corr}) in the case of the control is −537 mV versus SCE and the corresponding corrosion current
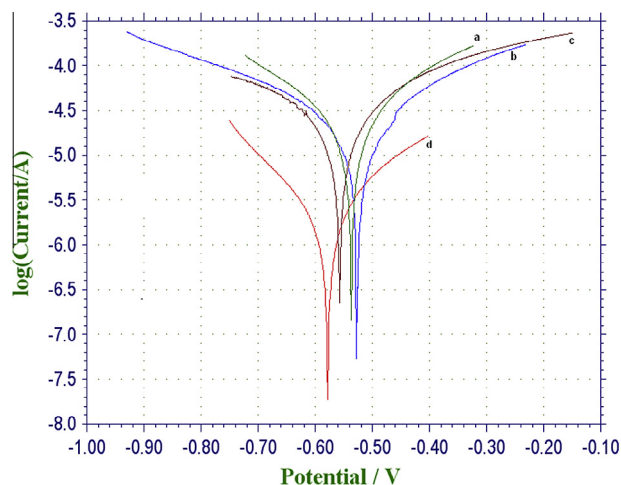
Figure 6b Potentiodynamic polarization curves of the mild steel immersed in various test solutions: (a) Control solution (60 ppm Cl^-); (b) 100 ppm IDMPA + 50 ppm Zn^{2+}.

density (I_{corr}) is 22.87 μA/cm^2. IDMPA alone shifts the E_{corr} value to a more anodic side. In the presence of IDMPA alone, the I_{corr} value is reduced slightly to 16.35 μA/cm^2. The shift in anodic Tafel slope (β_a) is greater than the shift in cathodic Tafel slope (β_c) in the presence of IDMPA alone. In literature reports [28,30], phosphonates in general are anodic inhibitors.

Table 3 Corrosion parameters of the mild steel immersed in the absence and in the presence of inhibitor obtained by potentiodynamic polarization studies.

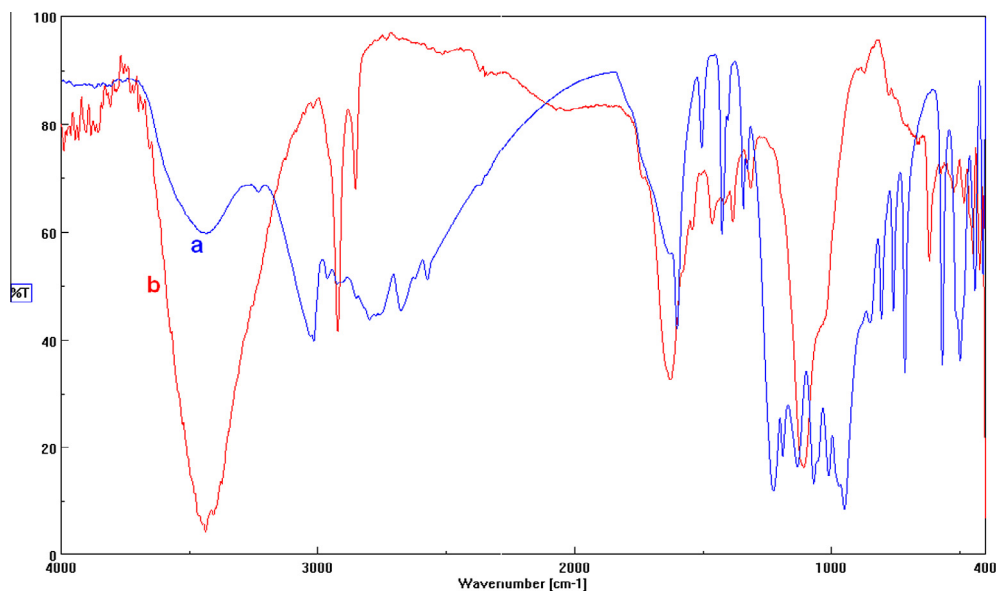| Concentration (ppm)		E_{corr} (mV vs SCE)	I_{corr} (μA/cm^2)	Tafel parameters		IE$_p$ (%)
IDMPA	Zn^{2+}			β_c (mV/decade)	β_a (mV/decade)	
0	0	−537	22.87	524	557	–
100	–	−528	16.35	480	632	29
–	50	−557	23.02	437	517	–
100	50	−578	2.28	667	580	90

Figure 7 FTIR Spectrum of (a) pure IDMPA (b) Surface film.

When Zn^{2+} is considered, the corrosion potential is shifted to the cathodic side and the shift in cathodic Tafel slope is greater. Contrary to the result obtained in the case of IDMPA, Zn^{2+} increased the rate of corrosion as implied by the increase in corrosion current density. Such an increase in corrosion rate in the presence of zinc ions alone was also reported in the literature [31]. From the polarization curves shown in Fig. 6, it is clear that the combination of IDMPA (100 ppm) and Zn^{2+} (50 ppm) significantly decreased corrosion current density values when compared to the control and also individual components. Thus, it is evident that this formulation acts as an effective mixed-type inhibitor. There is a slight shift in corrosion potential to a more cathodic side, and the shift in cathodic Tafel slope is greater than the shift in anodic Tafel slope. The corrosion current density is significantly decreased from 22.87 to 2.28 $\mu A/cm^2$, corresponding to an inhibition efficiency of 90%. Thus, the synergistic mixture of 100 ppm of IDMPA and 50 ppm of Zn^{2+} is proved to be an effective corrosion inhibitor for the mild steel. These results indicate that the binary inhibitor formulation retards both the anodic dissolution of the mild steel and oxygen reduction at cathodic sites in the corrosion inhibition process. Nevertheless, the effect on cathodic reaction is more pronounced. Similar phosphonate-based formulations were reported to be mixed inhibitors [32,33]. A significant observation related to the inhibition efficiency values is to be noted. If the inhibition efficiency values obtained from gravimetric (IE_g), polarization (IE_p), and EIS (IE_i) studies are compared, slight differences are observed. It is suggested that the inhibition efficiency values obtained from various methods may not be strictly comparable when the immersion times used in these methods are not the same [34].

3.4. Fourier transform infrared spectroscopy (FTIR)

The FTIR spectrum of KBr pellet of pure IDMPA is shown in Fig. 7a. The characteristic band of phosphonic acid is due to the associate P=O stretching vibration 1140–1380 cm^{-1} and another band symmetric/asymmetric P—OH stretching
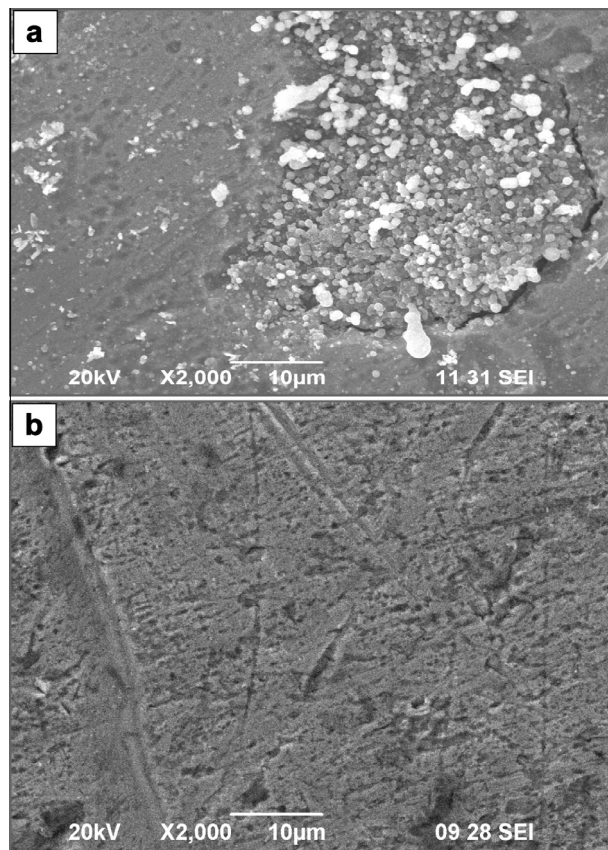

Figure 8 SEM images of (a) 60 ppm Cl⁻ (b) 60 ppm Cl⁻ + 100 - ppm IDMPA + 50 ppm Zn^{2+}.

vibrations at 1188–970 cm^{-1} has been reported [35]. The absorption peaks at 1020–580 cm^{-1}, indicate the corrosion products of Ferric hydroxide (γ-FeOOH) and magnetite (Fe_3O_4) respectively [36].

The pure IDMPA shows P=O stretching vibration at 1228.4 cm^{-1} and P—OH stretching vibration at 950 cm^{-1}. The broad absorption peak at 1602 cm^{-1} shows N—H stretching vibration. Carter et al. [37] found that FT-IR Spectra obtained with an organic phosphonate on a steel substrate are consistent with the phosphonate reaction on steel to produce metal salt. This shows that the phosphonates are coordinated with the metal to form a metal phosphonate complex. The FT-IR spectrum of IDMPA with Zn^{2+} is shown in Fig. 7b. The P=O stretching vibration shifts from 1228.4 to 1106 cm^{-1}, the P—OH stretching has disappeared. The imine (N—H) stretching shows the shift from 1602 to 1629.5 cm^{-1}. The moderate and intense peak that appears at 3436 cm^{-1}, in case of a control can be assigned to the presence of the OH group on the surface. Some other peaks appear at 1020.16 cm^{-1} and 449.33 cm^{-1} that show the presence of (γ FeOOH) and Fe$_3$O$_4$ in the inhibited film. The peaks observed around 1384.64 cm^{-1} indicate the presence of zinc hydroxide in the surface film [38]. From the FTIR spectral studies the protective film formed on the metal surface may be due to the formation of Zn^{2+}–IDMPA complex and [Fe (II)–IDMPA] complex.

3.5. Scanning electron microscopy (SEM)

The surface image of the mild steel was examined in the presence and absence of inhibitor (IDMPA–Zn^{2+}). The SEM micrograph of the mild steel after exposure for 7 days in a
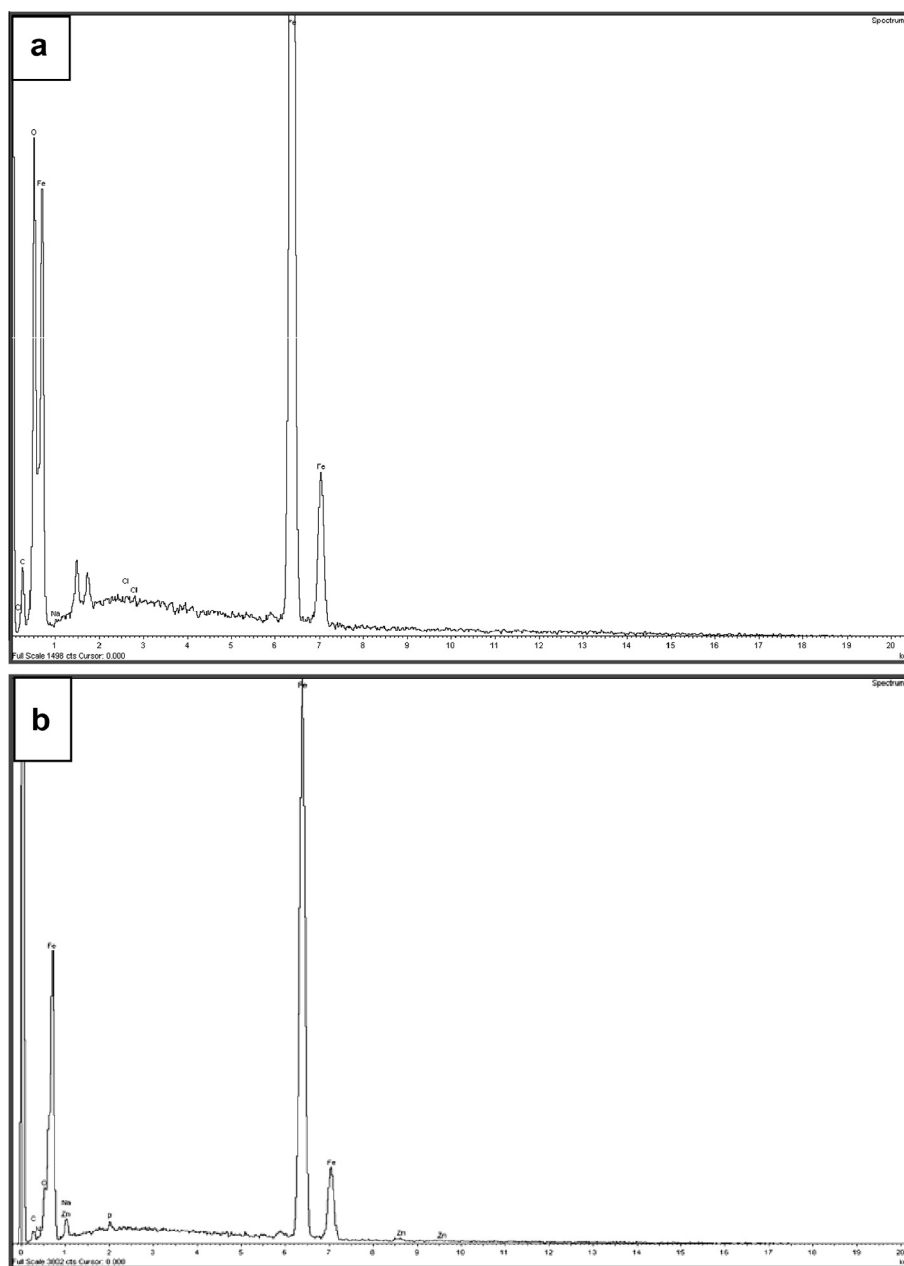
Figure 9   EDX survey spectrum is present in the mild steel surface (a) absence of inhibitor; (b) presence of inhibitor.

solution without inhibitor is shown in Fig. 8a. The image has several pits and cracks. The pits that appear in the image show that the metal was corroded severely and contains iron oxides as corrosion product. Several white patches seen in the image show the presence of some other form of corrosion products also.

The surface of the mild steel after the immersion of 7 days in aqueous solution containing 60 ppm Cl^-, 50 ppm Zn^{2+}, 100 ppm IDMPA is shown in Fig. 8b. It can be seen that the adsorbed film is formed and consequently retards the dissolution of metal. It is important to know that when IDMPA was present in the solution, the surface morphology of the mild steel is quite different from the previous one and the IDMPA forms some kind of complex with iron on the substrate. It may be concluded the SEM micrograph reveals that the surface film formed by the inhibitor system exhibits good inhibitive properties for the mild steel in aqueous environment.

3.6. Energy dispersive analysis of X-rays (EDX)

The protective film formed on the mild steel surface was analyzed using an energy dispersive analysis of X-ray technique (EDX) as shown in Fig. 9. EDX survey spectra were used to determine the composition of elements present in the mild steel surface before and after exposure to inhibitor solution. The spectrum in the case of the mild steel immersed in aqueous solution containing 60 ppm Cl^- without inhibitor as shown in Fig. 9a. The EDX analysis of the mild steel surface in chloride solution alone showed that the surface film contains mainly Fe with small percentages of C, Na, O and Cl. This shows that corrosion of iron takes place through the formation of iron oxide or iron chlorides.

On the other hand, the elements found in the adsorbed film obtained by EDS in the presence of the corrosion inhibitor (Fig. 9b) were C, Na, N, P, Fe, Zn, and O besides the iron substrate in addition to a very low content of chlorine. The appearance of low content of chlorine in the EDX confirms that inhibitor molecule precludes the corrosion of iron through its strong adsorption on the mild steel surface blocking its weak flaws and preventing the formation of ferrous and ferric chloride compounds. Therefore, the EDX and SEM examinations of the mild steel surface support the results obtained from the chemical and electrochemical methods that the inhibitor is a good inhibitor for the mild steel in aqueous solution. Similar reports have been observed in the literature [39].

3.7. Quantum chemical calculations

Quantum chemical calculations were performed to explain the relationship between the molecular structure and the inhibitive action of the inhibitors under study [40]. Quantum chemical parameters including the energy of the highest occupied/lowest unoccupied molecular orbital (E_{HOMO}/E_{LUMO}), the energy gap (ΔE) between HOMO and LUMO, and the molecular dipole (μ) are listed in Table 4. The charge distribution in a molecule can provide a critical insight into its physical and chemical properties. The map of the studied inhibitor is displayed in Fig. 10(a) and (b) shows the electrostatic potential that indicates the size and shape as well as charge distribution of the compound. Some quantum chemical parameters are related to the interactions between the inhibitor and the metal surface. E_{HOMO} is often associated with the capacity of a molecule to donate electrons. An increase in the value of E_{HOMO} can facilitate adsorption and thereby the inhibition efficiency, indicating disposition of the molecule to donate orbital electrons to an appropriate acceptor with empty molecular orbitals [41]. Therefore, E_{LUMO} indicates the ability of the molecule to accept electrons. The lower the value of E_{LUMO}, the more the probability that the molecule will accept electrons. Consequently, low absolute values of the energy band gap ($E_{HOMO} - E_{LUMO}$) will render good inhibition efficiencies, because the energy to remove an electron from the highest occupied orbital will be low [42].

The calculated quantum chemical parameters (Table 4) reveal that IDMPA has high HOMO and low LUMO, with a large energy gap. The calculated quantum chemical data include the energy of the highest occupied molecular orbital ($E_{HOMO} = -0.1756$ eV), energy of the lowest unoccupied molecular orbital ($E_{LUMO} = -0.082$ eV), dipole moment ($\mu = 7.0066$ D) and the energy gap, ΔE ($E_{LUMO} - E_{HOMO} = -0.0954$ eV). The high value of E_{HOMO} is likely to indicate a tendency of the molecule to donate electrons to the appropriate acceptor molecule with low energy and empty molecular orbital, whereas the value of E_{LUMO} indicates the ability of the molecule to accept electrons. Therefore, the value of ΔE provides a measure for the stability of the formed complex on the metal surface. In principle, a decrease in the energy gap leads to easier polarization of the molecule and greater adsorption on the surface [43]. Thus, a small ΔE in IDMPA facilitates adsorption, and enhances the efficiency of inhibition. The high inhibition efficiency of a molecule can be attributed to the high value of dipole moment and low value of ΔE. The results of the high dipole moment and the low energy gap indicate that electron transfer from IDMPA to the surface takes place during adsorption to the metal surface.

3.8. Mechanism of corrosion protection

A plausible mechanism of corrosion inhibition is proposed:
Mild steel undergoes initial corrosion to form Fe^{2+} ions at the anodic sites:

$$Fe \rightarrow Fe^{2+} + 2e^- \tag{7}$$

Fe^{2+} further undergoes oxidation in the presence of oxygen available in the aqueous solution:

$$Fe^{2+} \xrightarrow{[O_2]} Fe^{3+} + e^- \tag{8}$$

The corresponding reduction reaction at cathodic sites in neutral and alkaline media is

Table 4 Calculated quantum chemical properties of IDMPA.

| Compound	E_{HOMO} (eV)	E_{LUMO} (eV)	Dipole μ (Debye)	Solvation energy (kcal/mol)	ΔE (eV)
IDMPA	−0.1756	−0.0802	7.0066	−447.58	−0.0954
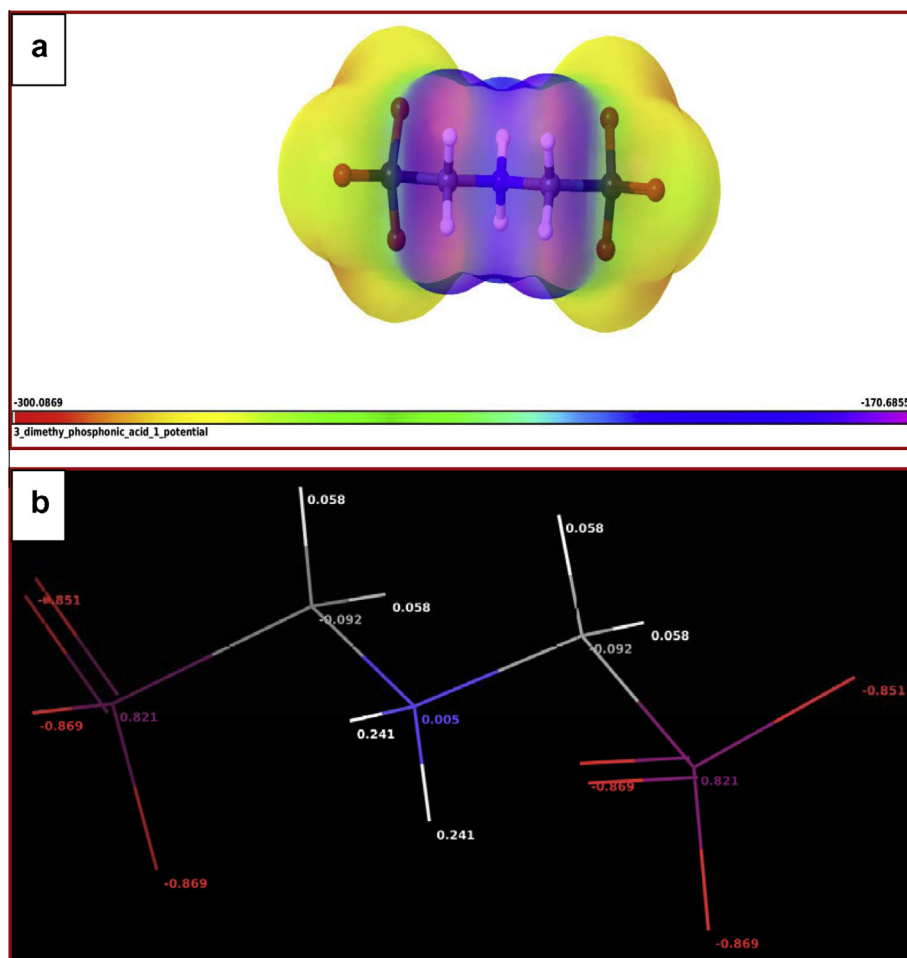
Figure 10 (a) Electrostatic potential map of the inhibitor; (b) Atomic charge distribution of IDMPA molecule.

$$O_2 + 2H_2O + 4e^- \rightarrow 4OH^- \qquad (9)$$

Fe^{2+} ions produced at anodic areas and OH^- ions produced at cathodic area combine to form $Fe(OH)_2$. Apart from $Fe(OH)_2$, there is formation of other oxides and hydroxides like FeOOH, γ-Fe_2O_3, etc., on the metal surface before the formation of the protective film.

When IDMPA and Zn^{2+} ions are added to the aqueous solution, IDMPA reacts with Zn^{2+} to form a complex [Zn(II)–IDMPA]. This complex diffuses to the metal surface and reacts with Fe^{2+}/Fe^{3+} ions available at the anodic sites to form [Fe(II)/Fe(III)/Zn(II)–IDMPA] complex which covers the anodic sites and controls the corresponding reaction at anodic sites:

$$[Zn(II)-IDMPA + Fe^{2+}/Fe^{3+}$$
$$\rightarrow [Fe(II)/Fe(III)/Zn(II)-IDMPA] \qquad (10)$$
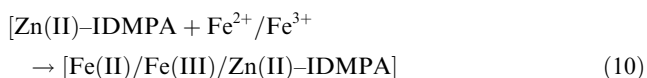
Free Zn^{2+} ions available in the bulk of the solution diffuse to the metal surface and react with OH^- ions produced at the cathodic sites to form a precipitate of $Zn(OH)_2$. This precipitate gets deposited on the cathodic sites and controls the cathodic reaction

$$Zn^{2+} + 2OH^- \rightarrow Zn(OH_2) \qquad (11)$$

Thus, IDMPA and Zn^{2+} play a very important role in the synergistic effect in controlling corrosion through the formation of a protective film on the metal surface.

4. Conclusions

Based on the above results, the following conclusion can be drawn:

1. All the measurements showed that the IDMPA–Zn^{2+} system has excellent inhibition properties for the corrosion of the mild steel in aqueous medium. The gravimetric measurements showed that the inhibition efficiency increases with increasing the concentration of IDMPA.
2. Potentiodynamic polarization measurements showed that the IDMPA acts as a mixed-type inhibitor predominantly cathodic nature. EIS measurements also indicate that the inhibitor concentration increases, with an increase in the charge transfer resistance and showed that the inhibitive property depends on adsorption of the molecules on the metal surface.
3. The binary inhibitor system Zn^{2+}–IDMPA affords good inhibition efficiency of 99%.
4. The inhibitor formulation Zn^{2+}–IDMPA is more effective in nearly neutral aqueous medium.

5. The inferences drawn from the results of EIS, potentiodynamic polarization and gravimetric studies are in good agreement.

6. The quantum chemical study shows that the nitrogen and oxygen atoms in the inhibitor molecule are the main active sites that result in adsorption of IDMPA on the mild steel surface.

7. It is concluded that the above formulations can be used in cooling water towers upon optimizing the concentrations and other conditions.

Acknowledgements

References

[1] A.M. Al-Sabagh, H.M. Abd-El-Bary, R.A. El-Ghazawy, M.R. Mishrif, B.M. Hussein, Egypt. J. Petrol. 20 (2011) 33–45.

[2] H.S. Awad, S. Turgoose, Corrosion 60 (2004) 1168–1179.

[3] S. Rajendran, B.V. Apparao, N. Palaniswamy, Electrochim. Acta 44 (1998) 533–537.

[4] E. Kalman, Working Party on Corrosion Inhibitors, vol. 11, EFC Publications, IOM Communications, 1994, p. 12.

[5] L.Y. Reznik, L. Sathler, M.J.B. Cardoso, M.G. Albuquerque, Mater. Corros. 59 (8) (2008) 685–690.

[6] E. Kalman, B. Varhegyi, I. Bako, I. Felhosi, F.H. Karman, A. Shaban, J. Electrochem. Soc. 141 (1994) 3357–3360.

[7] J.L. Fang, Y. Li, X.R. Ye, Z.W. Wang, Q. Liu, Corrosion 49 (1993) 266–271.

[8] D. Mohammedi, A. Benmoussa, C. Fiaud, E.M.M. Sutter, Mater. Corros. 55 (2004) 837–844.

[9] H. Amar, J. Benzakour, A. Derja, D. Villemin, B. Moreau, T. Braisaz, A. Tounsi, Corros. Sci. 50 (2008) 124–130.

[10] G. Gunasekaran, N. Palaniswamy, B.V. Apparao, Bull. Electrochem. 12 (1996) 59–63.

[11] S. Rajendran, B.V. Apparao, N. Palaniswamy, V. Periasamy, G. Karthikeyan, Corros. Sci. 43 (2001) 1345–1354.

[12] M. Prabakaran, M. Venkatesh, S. Ramesh, V. Periasamy, Appl. Surf. Sci. 276 (2013) 592–603.

[13] S. Rajendran, B.V. Apparao, N. Palaniswamy, Anti Corros. Methods Mater. 47 (2000) 147–151.

[14] H. Amar, J. Benzakour, A. Derja, D. Villemin, B. Moreau, J. Electroanal. Chem. 558 (2003) 131–139.

[15] K.D. Demadis, C. Mantzaridis, P. Lykoudis, Ind. Eng. Chem. Res. 45 (2006) 7795–7800.

[16] R. Touir, N. Dkhireche, M. Ebn Touhami, M. Sfaira, O. Senhaji, J.J. Robin, B. Boutevin, M. Cherkaoui, Mater. Chem. Phys. 122 (2010) 1–9.

[17] El. Sayed M. Sherif, Mater. Chem. Phys. 129 (2011) 961–967.

[18] K. Juttner, Electrochim. Acta 35 (1990) 1501–1508.

[19] H. Shih, F. Mansfeld, Corros. Sci. 29 (1989) 1235–1240.

[20] A. Alagta, I. Felhosi, J. Teleghi, I. Bartoti, E. Kalman, Corros. Sci. 49 (2007) 2754–2766.

[21] G. Gunasekaran, L.R. Chauhan, Electrochim. Acta 49 (2004) 4387–4395.

[22] M.S. Morad, Corros. Sci. 42 (2000) 1307–1326.

[23] F. Mansfeld, M.W. Kendig, W.J. Lorenz, J. Electrochem. Soc. 132 (1985) 290–296.

[24] G. Li, H. Ma, Y. Jiao, S. Chen, J. Serb. Chem. Soc. 69 (2004) 791–805.

[25] J. Ross Macdonald, J. Electroanal. Chem. 223 (1987) 25–50.

[26] K.F. Khaled, N. Hackerman, Electrochim. Acta 49 (2004) 485–495.

[27] I. Felhosi, Zs. Keresztes, F.H. Karman, M. Mohai, I. Bertoti, E. Kalman, J. Electrochem. Soc. 146 (1999) 961–969.

[28] Y. Gonzalez, M.C. Lafont, N. Pebere, F. Moran, J. Appl. Electrochem. 26 (1996) 1259–1265.

[29] M.A. Pech-Canul, L.P. Chi-Canul, Corrosion 55 (10) (1999) 948–956.

[30] X.H. To, N. Pébère, N. Pelaprat, B. Boutevin, Y. Hervaud, Corros. Sci. 39 (1997) 1925–1934.

[31] S. Rajendran, B.V. AppaRao, N. Palaniswamy, Bull. Electrochem. 17 (2001) 171–174.

[32] M.A. Pech-Canul, P. Bartolo-Perez, Surf. Coat. Technol. 184 (2004) 133–140.

[33] M. Prabakaran, S. Ramesh, V. Periasamy, Res. Chem. Intermed. (2012), http://dx.doi.org/10.1007/s11164-012-0858-5.

[34] B.V. Apparao, M. Venkateswararao, S. Srinivasarao, B. Sreedhar, J. Chem. Sci. 122 (2010) 639–649.

[35] N.B. Colthup, L.H. Daly, S.E. Wiberley, Introduction to Infrared and Raman Spectroscopy, third ed., Academic press, New York, 1990.

[36] K. Nakamoto, Infrared and Raman Spectra of Inorganic and Co-ordination Compounds, fourth ed., John Wiley & Sons, New York, 1986.

[37] R.O. Carter, C.A. Gierczak, R.A. Dickie, Appl. Spectrosc. 40 (5) (1986) 649–655.

[38] I. Sekine, Y. Hirakawa, Corrosion 42 (1986) 272–277.

[39] M.A. Migahed, M.M. Attya, S.M. Rashwan, M. Abd El-Raouf, A.M. Al-Sabagh, Egypt. J. Petrol. 22 (2013) 149–160.

[40] A.M. Al-Sabagh, N.M. Nasser, A.A. Farag, M.A. Migahed, A.M.F. Eissa, T. Mahmoud, Egypt. J. Petrol. 22 (2013) 101–116.

[41] A.M. Al-Sabagh, N.Gh. Kandil, O. Ramadan, N.M. Amer, R. Mansour, E.A. Khamis, Egypt. J. Petrol. 20 (2011) 47–57.

[42] A.Y. Musa, A.A.H. Kadhum, A.B. Mohamad, M.S. Takriff, A.R. Daud, S.K. Kamarudin, Corros. Sci. 52 (2010) 526–533.

[43] A.S. Fouda, A.S. Ellithy, Corros. Sci. 51 (2009) 868–875.